이학석사학위논문

Time-Resolved Spectroscopic Study of Charge Transfer Dynamics of Quantum Dots and Au-rod-TiO_2 Nanocomposite

시분해 분광기술을 이용한 양자점과 금 로드-산화티타늄의
전하 이동 동역학 연구

2013년 2월

서울대학교 대학원

화학부 물리화학전공

황 선 진

MS. Dissertation

Time-Resolved Spectroscopic Study of Charge Transfer Dynamics of Quantum Dots and Au-rod-TiO_2 Nanocomposite

Sunjin Hwang

Research Advisor: Professor Seong Keun Kim

Department of Chemistry

Seoul National University

Time-Resolved Spectroscopic Study of Charge Transfer Dynamics of Quantum Dots and Au-rod-TiO_2 Nanocomposite

시분해 분광기술을 이용한 양자점과 금 로드-산화티타늄의
전하 이동 동역학 연구

지도교수 김 성 근
이 논문을 이학석사학위논문으로 제출함

2013년 2월

서울대학교 대학원

화학부 물리화학전공

황 선 진

황선진의 이학석사학위논문을 인준함
2013년 2월

위 원 장 서 정 쌍 (인)
부위원장 김 성 근 (인)
위 원 신 석 민 (인)

Abstract

Time-Resolved Spectroscopic Study of Charge Transfer Dynamics of Quantum Dots and Au-rod-TiO_2 Nanocomposite

Sunjin Hwang

Department of Chemistry

The Graduate School

Seoul National University

Time resolved spectroscopic technique has been applied for study of photo physical properties and photo dynamics of transient species. This technique has its own distinct advantage which enables us to study transient species including excited states, intermediates and transition state. The focus of this work has been probed in charge transfer dynamics and carrier relaxation of QDs and semiconductor by time resolved spectroscopic techniques which are fully employed to study and understand excited state dynamics and their novel chemical properties.

Quantum dots are tiny particles, or “nanoparticles”, of a semiconductor material, traditionally chalcogenides (selenides or sulfides) of metals like cadmium or zinc (CdSe or ZnS, for example), which range from 2 to 10 nanometers in diameter. Because of their small size, quantum dots display unique optical and electrical properties that are different in character to those of the corresponding bulk material. Moreover, the wavelength of emissions depends not on the composition of the quantum dot, but its size. Quantum dots can therefore be “tuned” during production to emit any color of light desired by changing its size. We synthesized a new highly QDs using multi shell structures and investigated its stability and photo properties. Passivation of QDs such as InP is reported to increase the quantum efficiency and stabilize its structure by protecting the core from external environments. We verified the charge transfer dynamics of InP QDs passivated with GaP and ZnS shell by using time-correlated single photon counting spectroscopy.

Semiconductor and metal nanoparticles display unique size dependent photo physical, electrochemical, photo catalytic and optical properties. The presence of metal facilitates electron transfer from photo excited semiconductor to the surroundings and decreases recombination rate between the electrons-holes in the semiconductor. The focus of this work provides mechanistic explanation for the size-dependent charge recombination rate of TiO_2 and Au rod/TiO_2 composite in UV region. We have found that the TiO_2 shell thickness and Au rod have influenced the charge recombination of TiO_2 by transient absorption spectroscopy.

Keywords: Transient absorption spectroscopy, Time-correlated single photon counting technique, quantum dots, TiO_2 semiconductor

Student Number: 2011-20314

Table of Contents

1. Introduction

Time-resolved spectroscopy is the name given to a set of experimental tools that allows for the measurement of time-resolved quantities. This technique has a wide range of application areas, including test and measurement in the semiconductor industry, materials characterization, biological analysis, and photo physical studies. One of the most popular and powerful pump-probe techniques is transient absorption (TA) spectroscopy; femto-TA is a pump-probe time-resolved optical spectroscopy technique of widespread application for the study of ultrafast processes. This technique provides a large amount of potential information regarding the dynamics and the nature of the elementary reactions that control the macroscopic properties of photosystems and the influence of the environment at the nanometer scale. Indeed, femto-TA can follow elementary processes such as solvation, chemical reaction, conformational change, excitonic energy or electron transfer in solution and solid state. Thus, this technique has been employed to reveal the spectra dynamic properties of photochemical and photo biological systems.

The other time resolved technique is time correlated single photon counting(TCSPC) spectroscopy which is most sensitive technique to measure the luminescence lifetime of luminescent compounds. The TCSPC setup uses picosecond pulsed LEDs or lasers and has a temporal resolution of tens of ps.

In this study, we used various time resolved time resolved spectroscopic techniques; transient absorption spectroscopy (TA) and time correlated single photon counting spectroscopy (TCSPC). By applying these techniques, we probed photo dynamics of Quantum dots (QDs) and semiconductor. We tried to understand the charge transfer dynamics and analyzed the correlation between lifetime and its dynamics.

2. Basic Principles

2.1 Transient Absorption Spectroscopy

Time-resolved transient absorption spectroscopy is a sensitive technique to study the time evolution (kinetics) of the excited states and the lifetimes of short living species by measuring the time dependent transient absorption signal.[1,2] In a typical pump-probe transient absorption experiment, two ultra-short laser pulses are irradiated on a sample in which they spatially overlap. The pump pulses are obtained using the sum and difference frequency shifting technique, whereas the spectrally broad probe pulses are obtained using the generation of white light continuum. Transient absorption signals are obtained by calculating ΔOD which is defined as ΔOD = OD (pump on) – OD (pump off). By varying the time delay (τ), a full time profile for the transient absorption can be acquired. This profile contains the information on the dynamical process under study, such as energy migration, charge/hydrogen transfer, isomerization and intersystem crossing.[3] This concept is graphically represented in Figure 1.

In general, the observed TA spectra consist of three contributions: ground state bleach (GSB), stimulated emission (SE) and excited state absorption (ESA). Ground state bleaching is instantaneous. A certain amount of the molecule in their ground state is promoted to their excited state. Therefore, after excitation, the probe beam will be less absorbed in the spectral range of the ground state absorption and will lead to negative OD (ΔOD<0). Stimulated emission, which is the molecules in the excited state, can relax to their ground state with the emission of light (ΔOD<0) if the probe beam possesses the specific energy. This signal is generally observed in the same wavelength range than the stationary fluorescence.[4] The third contribution is provided by excited-state absorption.

Upon excitation with the pump beam, optically allowed transitions from the excited states to higher excited states may exist in certain wavelength regions, and absorption of the probe pulse at these wavelengths will occur. Consequently, a positive signal is observed in the wavelength region of excited-state absorption (ΔOD>0).

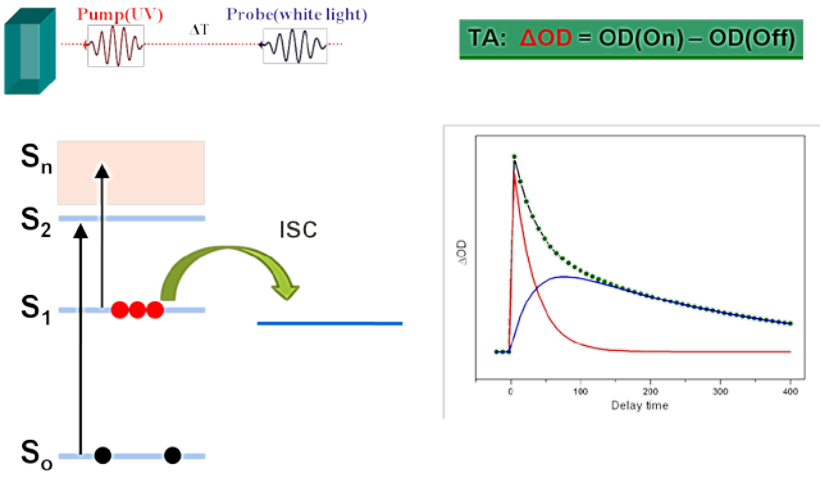

Figure 1. Graphical representation of transient absorption spectroscopy.

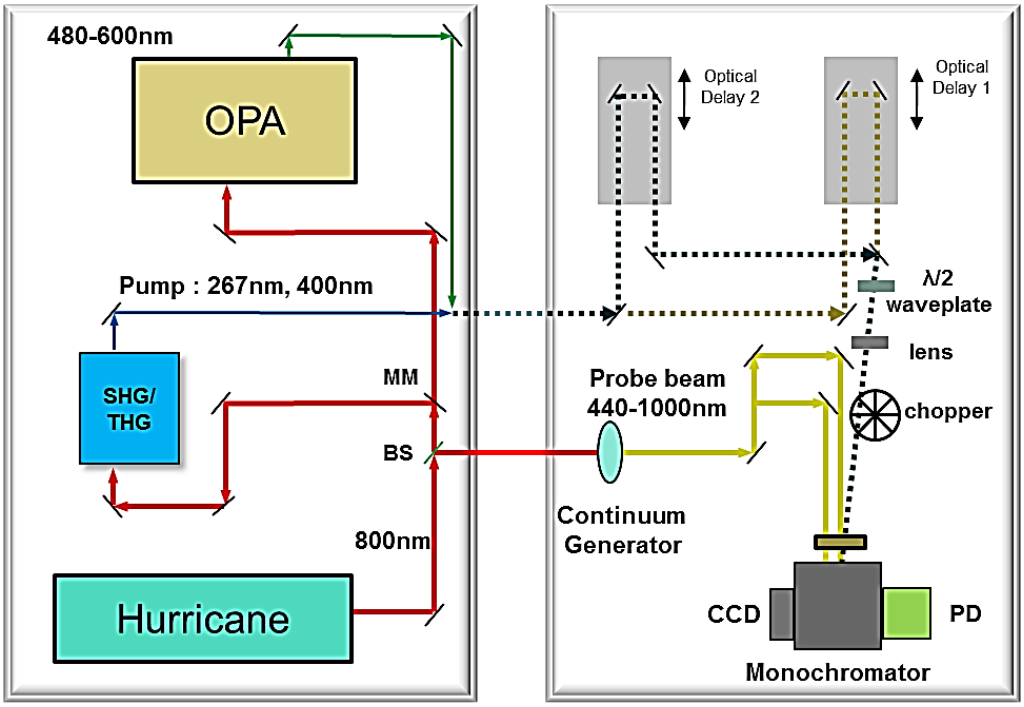

Figure 2. Graphical representation of experimental setup for TA spectroscopy.

2.2 Time-Correlated Single Photon Counting Spectroscopy

The main purpose of TCSPC technique is to measure the fluorescence lifetime of a sample. The sample is first excited with a pulse laser, usually in the range of picoseconds or femtoseconds, and then the first photon emitted is detected by a photomultiplier tube (PMT) or avalanche photodiode (APD). The arrival time of the detected photon is recorded as one event. After detection of a large number of photons, the distribution of the photons over a range of arrival time can be plotted. The x-axis is the time and the y-axis is the number of photons detected at a particular time period. At each excitation, one photon or less than one photon is detected because electronics is not fast enough for multiple detection of photons when the lifetimes of the samples are in the nanosecond range. Moreover, when the lifetime of the sample is in the picosecond range other spectroscopic techniques such as fluorescence up-conversion spectroscopy must be employed. [5, 6]

3. Trap Site of Semiconductor Nanocrystals-dependent Charge Transfer Dynamics

3.1 Introduction

Quantum dots are spherically shaped semiconductor crystalline particles with a dimension comparable with or smaller than the exciton size in the respective bulk semiconductor.[7] It is also referred to as semiconductor nanocrystal (NC) due to its nanometer sized structure dimension.[8]

Synthesis of type-I semiconductor nanocrystal was studied in relation to its various applications ranging from bio-imaging to light-emitting diodes. However, core quantum dots have one major flaw, in which their fluorescence showed an occasional blinking perhaps partly prompted by the contact with the surrounding environment.[9] The efficiency of semiconductor quantum dot has recently been improved by passivation of the core structure, [10] which suppresses the emission from trap sites. Indium phosphide (InP) is less toxic than cadmium selenide (CdSe)[11] and has a broad photoluminescence emission in the visible range. A significant increase in the quantum yield of both InP/Zn, which is etched on InP core structure, and InP/ZnS core-shell structure has been previously reported.[12]

However, these core shell structures were prone to photochemical oxidation, and therefore a new solution was needed to overcome this limitation. Recently, it was reported that Gallium Phosphide (GaP) reduced the effect of lattice mismatch between InP core and ZnS shell which led to a significant increase in photochemical stability. We measured TEM images which showed a size change, and tested stability of InP/GaP/ZnS QDs upon high temperature and UV light.

We consequently have found that InP/GaP/ZnS QD has better stability because of the GaP shell. We also verified the passivation-induced improvement in quantum yield by photoluminescence spectrum. We try to understand the charge transfer dynamics which depend on the condition of lattice mismatch by time-correlated single photon counting (TCSPC).

3.2 Results and Discussion

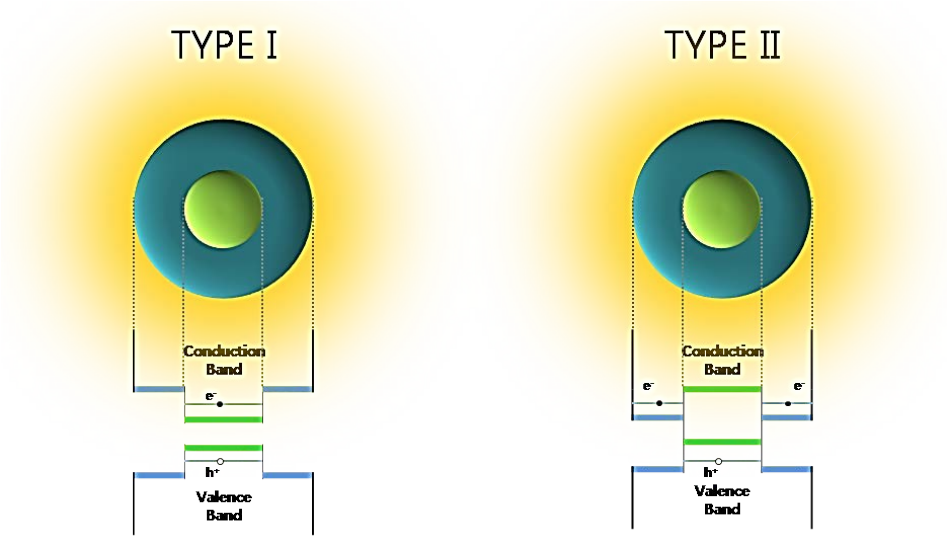

Figure 3. Graphical representation for different types of core-shell quantum dots.

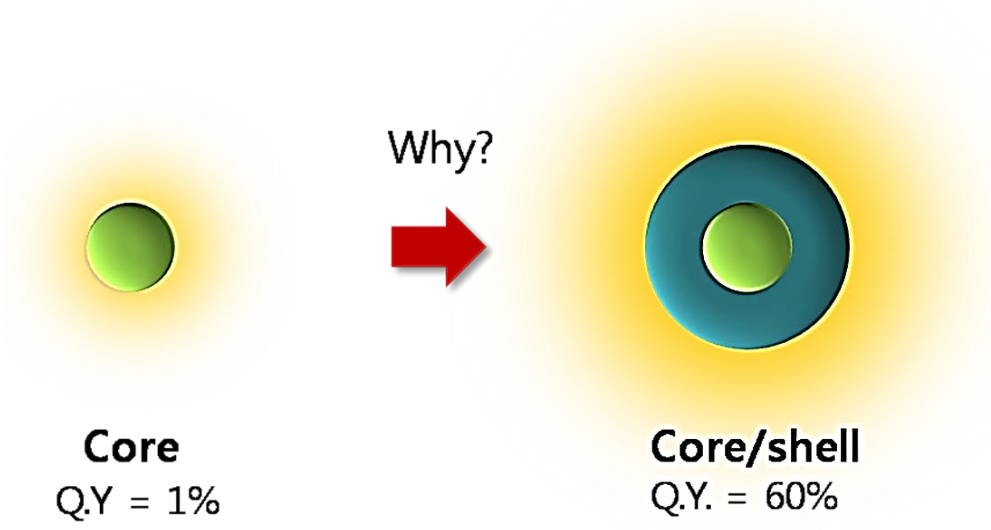

Figure 4. Graphical representation for passivation of QDs.

In general, core-shell quantum dots can be divided into different functions depending on the functions of the shell.[13] The main difference is in the level as well as the size of the band gap of the materials. In the first type, the band gap of the shell is larger than the core (Figure 3). Thus, when photo excitation occurs, the electrons and holes will be confined to the core. For the second type, the band gap of the shell is smaller and lower than the core which will result in lesser confinement of the exciton in the core.

We used the stepwise synthesis of InP/ZnS core-shell quantum dots and the role of zinc acetate during the reaction. Zinc acetate was used as a precursor for zinc and acetic acid. Highly luminescent InP/Zn was obtained as an intermediate. The InP core was synthesized with indium acetate (In(OAc)3), tris(trimethylsilyl)phosphine ((TMS)3P), and palmitic acid as the indium and phosphorus precursors and stabilizers, respectively, using the methodology reported in Peng and Battaglia's paper.[14] Below scheme is represented for stepwise InP to InP/ZnS.

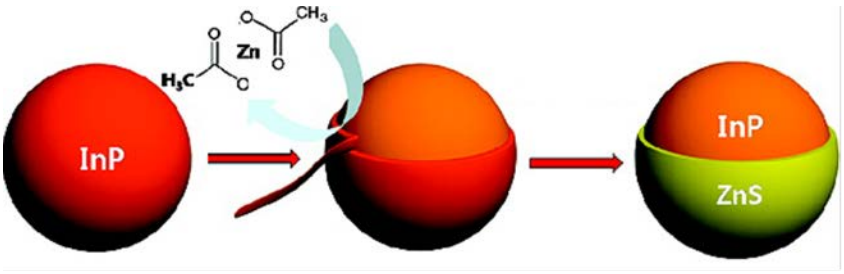

Figure 5. Schematic represent for InP to InP/ZnS

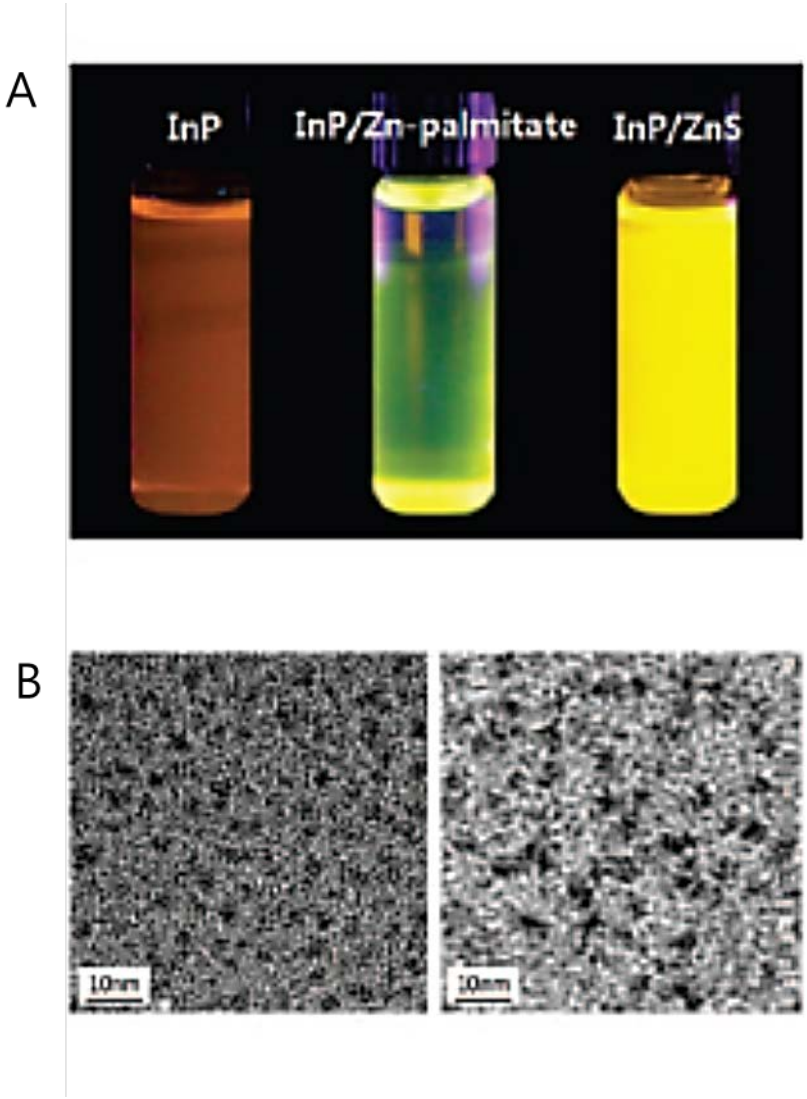

Figure 6. (A) Photograph of InP, InP/ Zn, and InP/ZnS NCs under UV. (B) TEM images of InP cores (left) and InP/ZnS core-shell (right).

Figure 6 (A) shows the photographs of the InP cores (left), InP/Zn (center) solutions and InP/ZnS (right) after cooling. Transmission electron microscopy (TEM) revealed InP cores and InP/ZnS core-shells, 2.9 nm and 3.5 nm in diameter, respectively (Figure 6B).

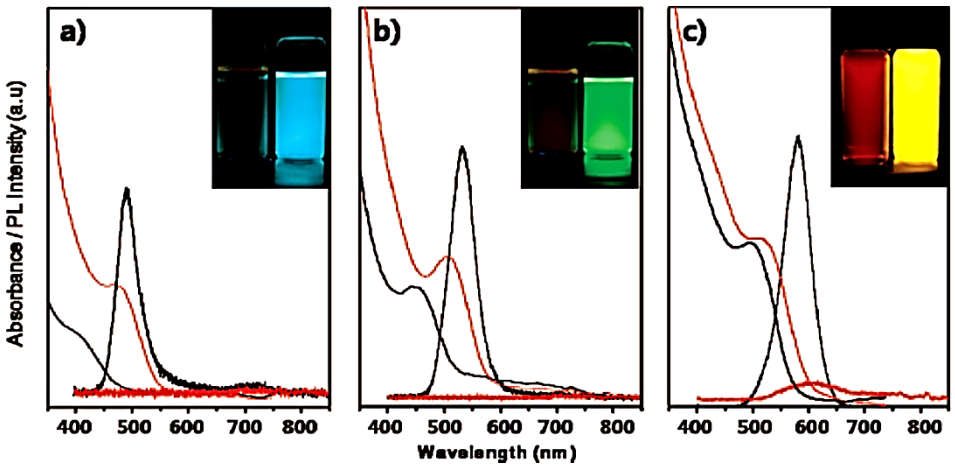

Figure 7. Photoluminescence and absorbance of InP cores (red) and InP/ZnS core shells (black) at each wavelength. Insets show the photograph of InP (left) and InP/ZnS (right) under UV, respectively.

Figure 7 shows the absorption and photoluminescence of the InP cores, and InP/ZnS core-shells solutions at each wavelength. There is significant blue shift in absorption and emission spectra between InP cores and InP/ZnS core shells. This blue shift is attributed to etching by acetic acid, which originated from zinc acetate, and was similar to HF etching.[15] Because original emission is from InP core, radius reduction of InP could affect its own emission. Also, this etched surface of core shell leads to the easy formation of core shell. The blue shift of absorption and emission could be explained by quantum confinement effects.[16]

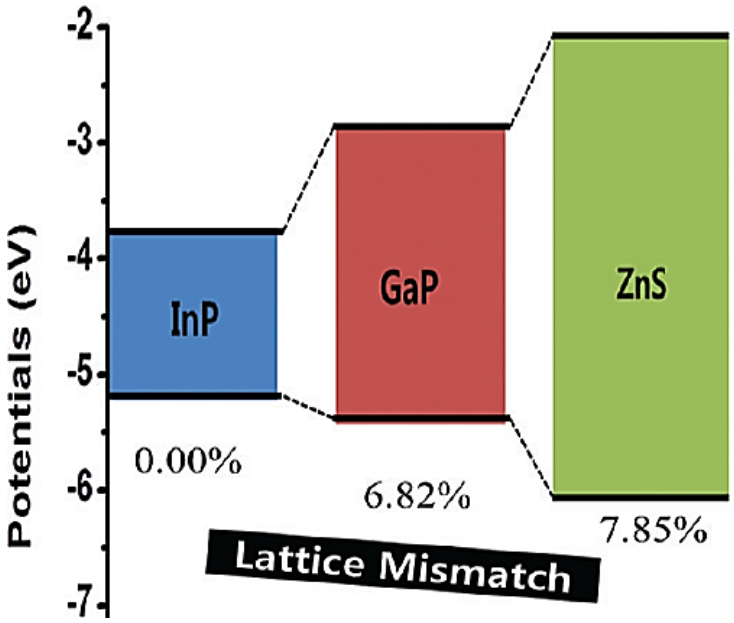

Figure 8. Band offsets and lattice mismatch of InP, GaP, and ZnS core/shell/shell materials.

InP QDs were synthesized by using a set of precursors and stabilizer such as zinc acetate ($Zn(OAc)_2$), indium acetate ($In(OAc)_3$), tris(trimethylsilyl)phosphine ($(TMS)_3P$), and palmitic acid (PA). Octadecene (ODE) solution of $Zn(OAc)_2$, $In(OAc)_3$, and PA was prepared, and a (TMS)3P−ODE stock solution was rapidly injected at 300 °C. As a result, the QY increased to 15% because the Zn^{2+} ions attached to the surface and partially removed the surface traps. The main source of GaP shell was from gallium-oleate complex solution.

We suggest a type-I structured InP/GaP/ZnS core/shell/shell QD. With the band gap of bulk GaP located between InP and ZnS, our QD forms a type-I structure (Figure3). The inner shell of GaP mitigates the effect of lattice mismatch between the InP core and the ZnS outer shell.

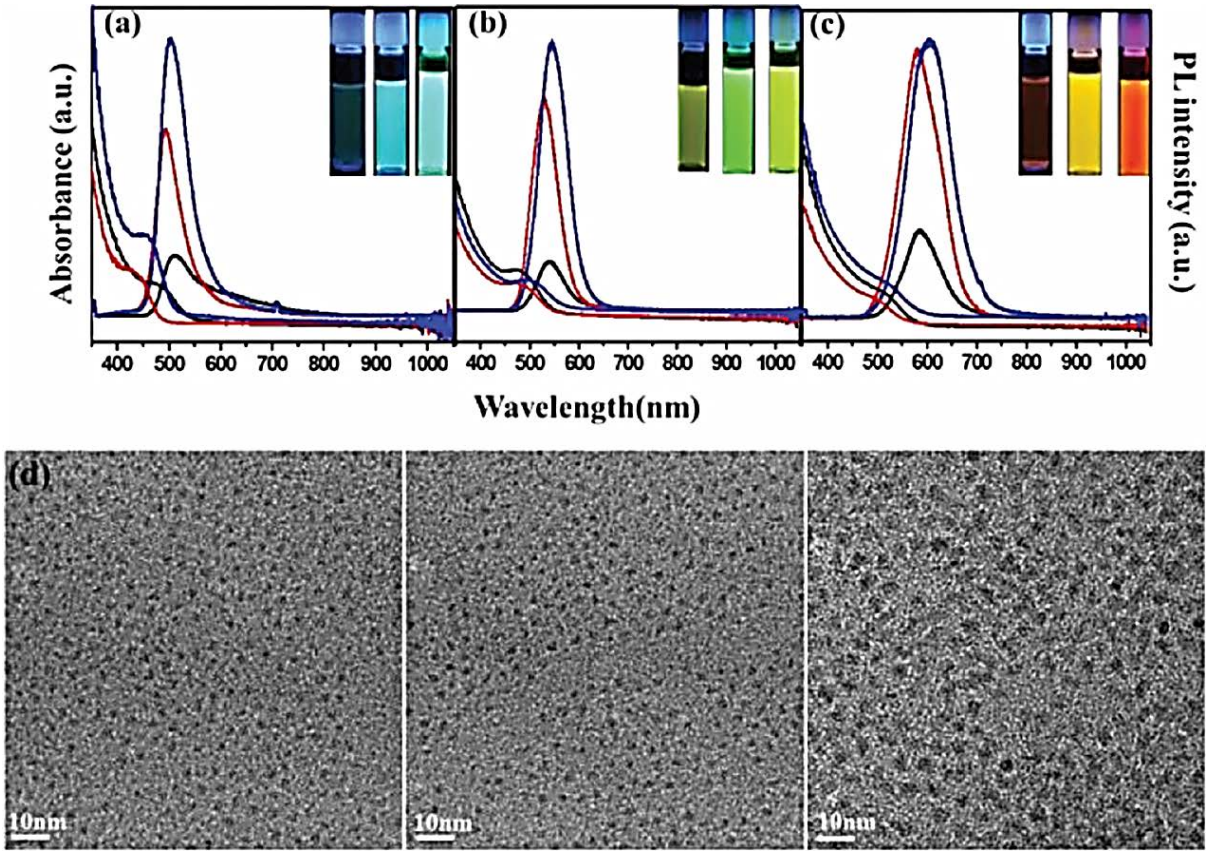

Figure 9. Absorption and photoluminesence spectra of InP (black) cores, InP/GaP (red) core−shells, and InP/GaP/ZnS (blue) core−shell−shell at each wavelength. Insets: Photograph of InP (left), InP/GaP (middle), and InP/GaP/ZnS (right) (a−c). (d) TEM image of InP (left), InP/GaP (middle), and InP/GaP/ZnS (right).

In this experiment, InP cores have three emission peaks at 515, 540 and 590nm. These InP cores were used to synthesis of InP/GaP and InP/GaP/ZnS core shells. By adding a Ga−oleate solution, we observed a blue shift of 5−15 nm in emission so that the peaks shifted to 490, 530, and 585 nm, respectively (Figure 9a−c). The absorption peaks were also blue-shifted.

This phenomena could be explained by a cation exchange[17] reaction between In^{3+} and Ga^{3+}, though the cations were different. We noted that similar phenomena have been reported previously.[18]

A cation exchange (Scheme 1) is likely to take place because of their common zinc-blende structures of similar lattice parameters (InP, 5.86 Å; GaP, 5.45 Å), and the similar ionic radius of Ga^{3+} (0.75 Å) and In^{3+} (0.81 Å). Suppose that Ga^{3+} ions effectively replace In^{3+} ions near the surface, a structurally reduction in size of the InP core after coating with a GaP shell due to a cation exchange can explain the blue shifts in emission and absorption.

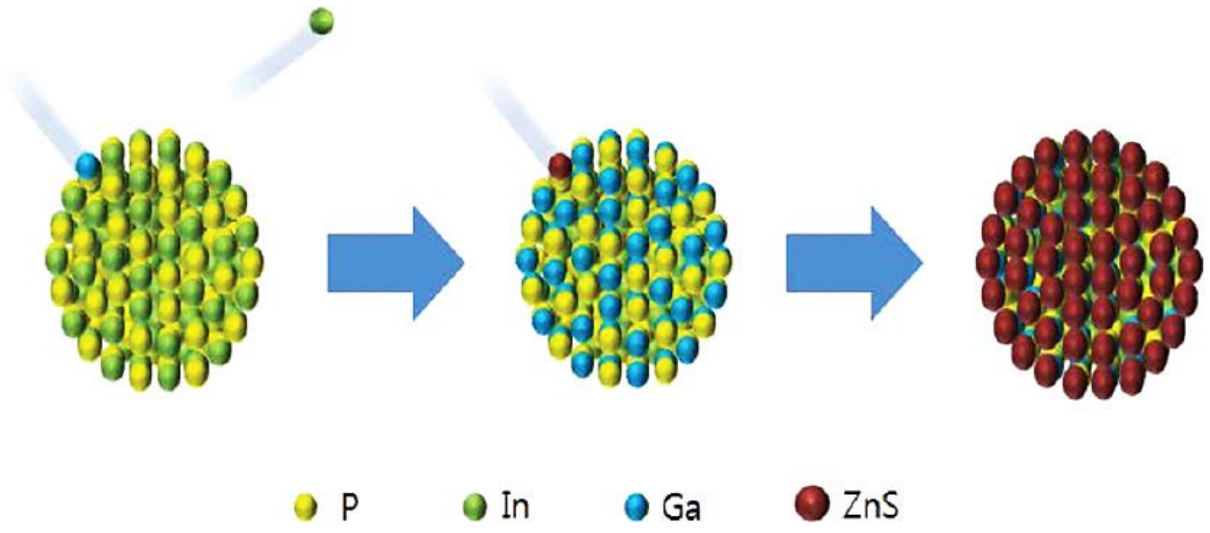

Scheme 1. Cation Exchange by Ga3+ on InP Core Surface

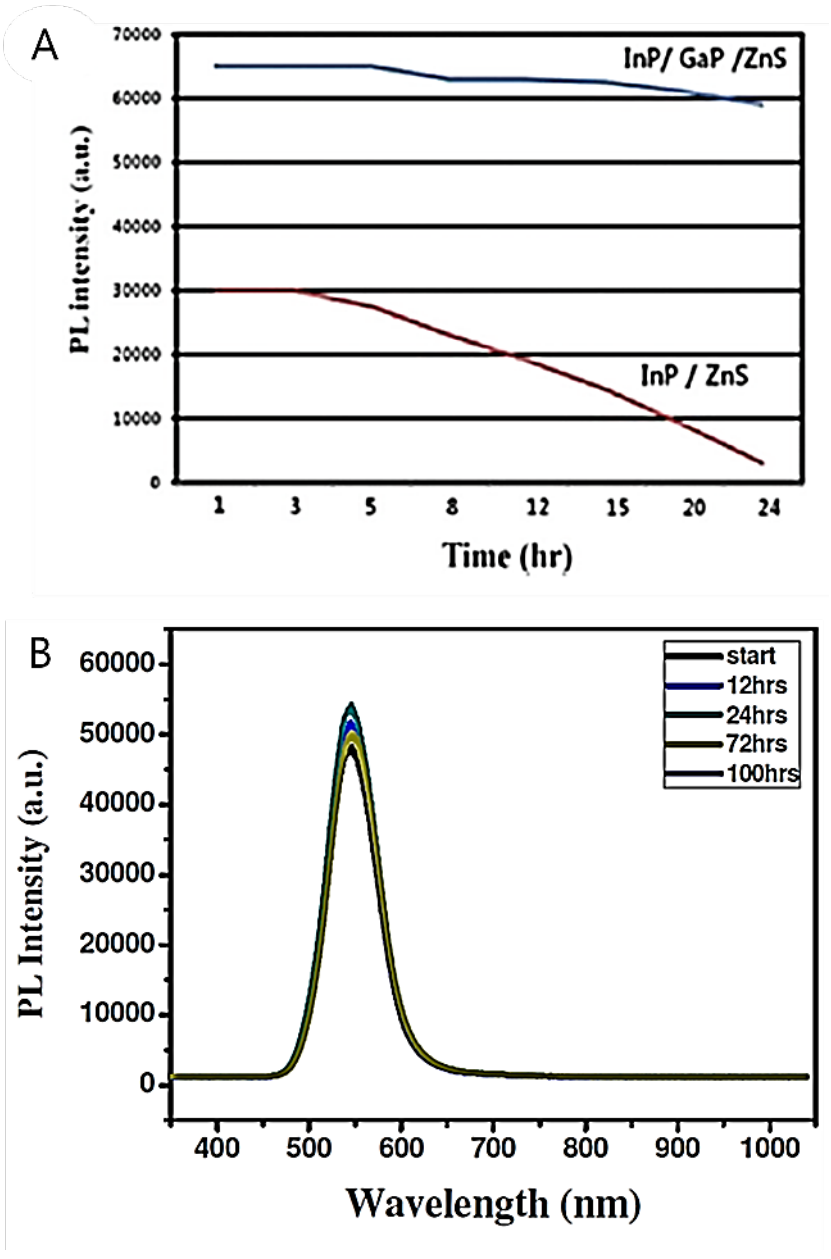

Figure 10. (A) Thermal stability of the InP/ZnS and InP/GaP/ZnS, which were tested at 150 °C. (B) UV test data of InP/GaP/ZnS NCs in hexane.

We examined the heat stabilities of InP/ZnS and InP/GaP/ZnS QDs by the change in photoluminescence (PL) intensity over time dependent on thermal treatment at 150 °C. Figure 10 A shows that the PL intensity of the InP/GaP/ZnS QDs decreased only a little (by ～10% in 24 h), while the InP/ZnS QDs showed a large decline after 3 h and by more than 90% in 24 h. This proves that our multishell QDs of InP/GaP/ZnS have a superior thermal stability compared with InP/ZnS QDs that were synthesized by our previously reported method.[11]

We also measured the PL intensity change of the InP/GaP/ZnS QDs under irradiation with a 254 nm UV lamp at a small distance of 10 cm for 100 h. No significant changes were detected in the PL intensity during this time (Figure 10 B), which again confirms that our multishell structure has good stability.

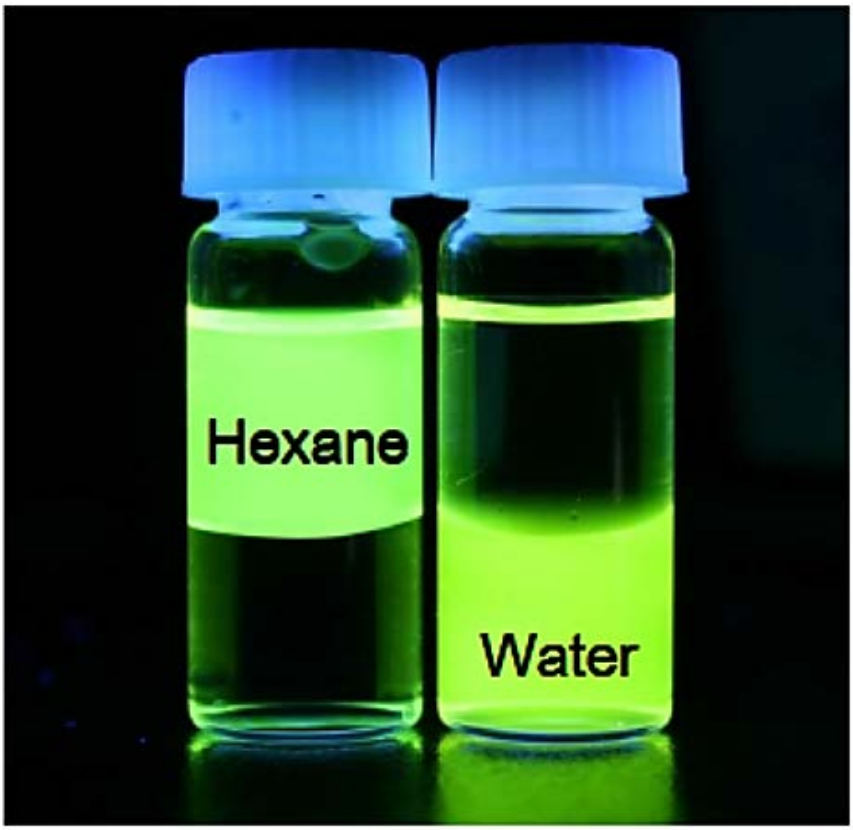

Figure 11. Photographs of InP/GaP/ZnS NCs in hexane (left) and water (right).

We were also able to transfer the QDs from an organic to an aqueous phase by ligand exchange, which produced highly luminescent and water-dispersible QDs (Figure 11).

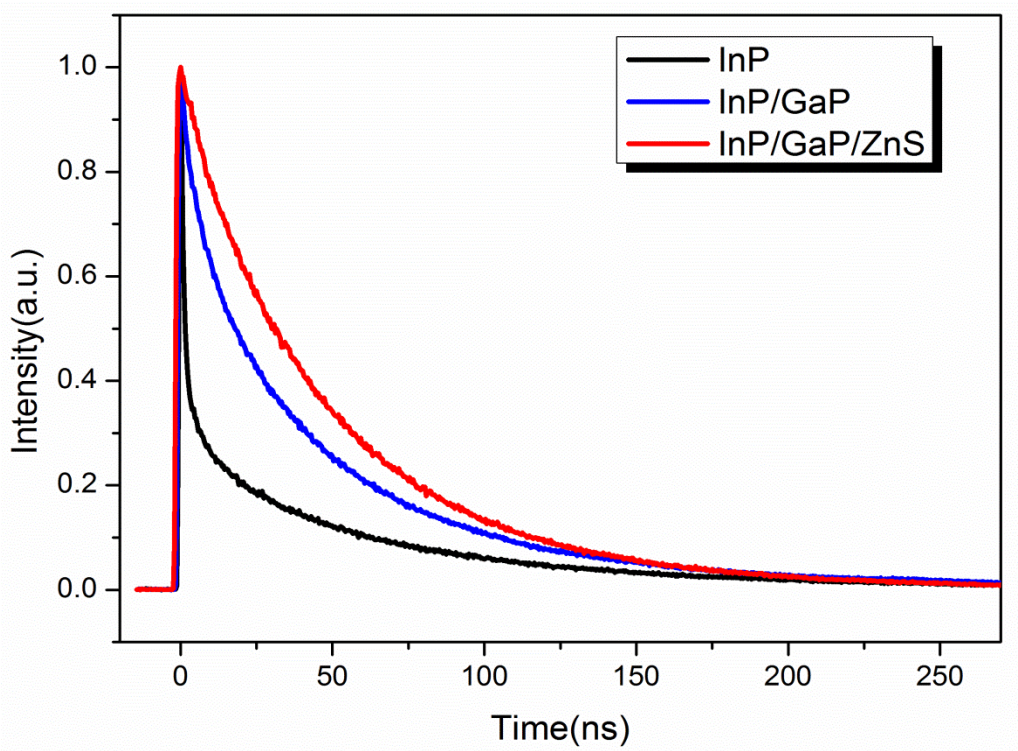

	$\tau_{1\ (ns)}$	$\tau_{2\ (ns)}$
ZnInP	1.4(70%)	52.3(30%)
ZnInP/GaP	6.9(32%)	50.9(68%)
InP/GaP/ZnS	13.6(12%)	52.2(88%)

Figure 12. TCSPC data of InP, InP/GaP, InP/GaP/ZnS.

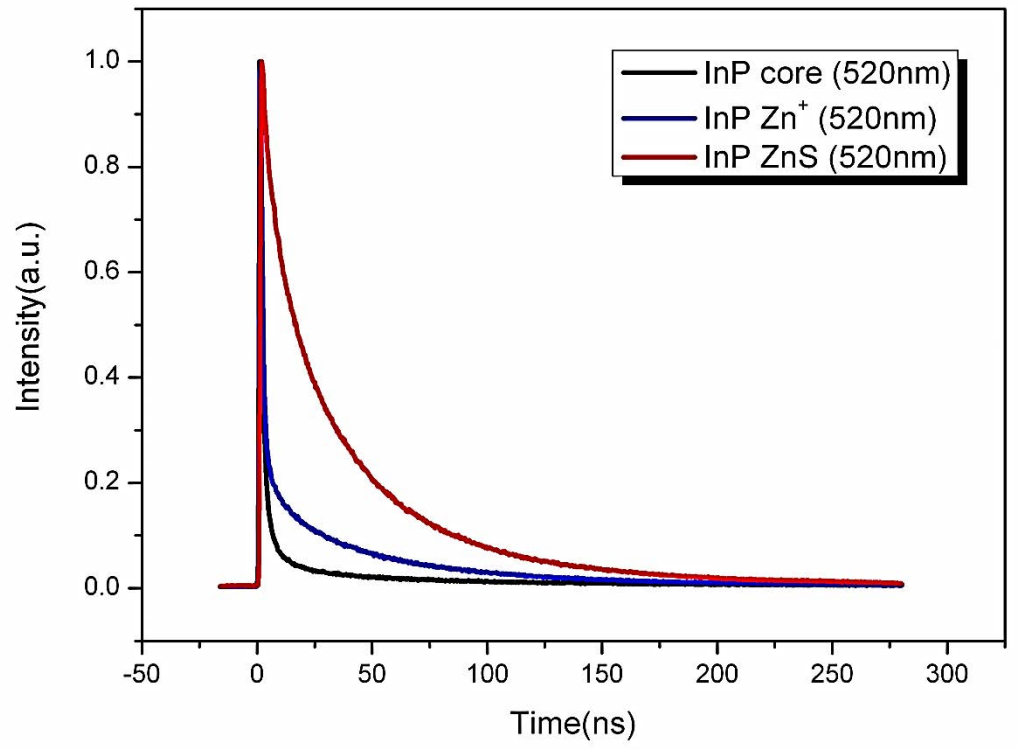

	$\tau_{1\ (ns)}$	$\tau_{2\ (ns)}$
InP	1.5(93%)	28.5(7%)
InP/Zn^{+}	1.1(80%)	40.3(20%)
InP/ZnS	7.4(37%)	43.1(63%)

Figure 13. TCSPC data of InP, InP/Zn^{2+}, and InP/ZnS.

In order to investigate the dynamical features of our QDs, we probed the temporal decay of the photo excited state by time-correlated single photon counting (TCSPC). Figure 12 represents TCSPC decay curve of InP, InP/GaP and InP/GaP/ZnS. Each QD was excited at 405nm wavelength and emission of QDs was fixed at 520nm wavelength. Fluorescence decay curves of QDs were fitted with bi exponential function and the fitting parameters are given in Figure 12 and 13:

$$f(t) = a1\exp^{(-t/t1)} + a2\exp^{(-t/t2)}, \text{ where } a1 + a2 = 1$$

We calculated that the amplitude for fast and slow decay component of QDs. The Figure 12 shows the tendency of slow component upon structures of core to multi-shell. The lowest for InP core (0.30) is observed, but increases drastically for the InP/GaP core/shell (0.68), and even further for the InP/GaP/ZnS core/shell/shell structure (0.88), which is explained by increment in fluorescence intensity as shell passivation increased. In general, the surfaces of colloidal QDs play important roles in carrier relaxation and recombination processes[19]. The carrier quenching defects on the surface can be minimized by shell passivation, thus the rate of radiative recombination is increased from localized surface sates. For quantum dots with core/shell structures, the atoms of the core and the shell epitaxially bond together with minimal defects.[20d] The individual LUMO of core and shell will have strong interactions, in which the core/shell LUMO will be largely delocalized throughout the reconstructed structure.[20d]

On the other hand, the tendency of fast decay component is opposite which is related to facile decay of carrier population because of the internal core state recombination. [20a, 21] One possible hypothesis is that the hole could be excited to the surface localized states at the same energy as that of the internal core states because of their strong mixing. [20a, 21] The average lifetime of the fast component was gradually risen as the passivation of InP increased due to the strong mixing of hole and surface states.

Figure 13 reports another comparative study about InP, InP/Zn^{2+} and InP/ZnS QDs which are intermediates for InP/ZnS core/shell QDs, and measured by TCSPC. We found that the amplitude of the slow component is larger for InP/Zn and largest for InP/ZnS, just as in the cases of InP/GaP and InP/GaP/ZnS, which again proves that passivation decreases the surface defects. It is also interesting that InP/Zn has a high contribution of fast component (0.80), whereas InP/GaP has a high contribution of slow component (0.68), which verified they are dissimilar structures. As a result, the formal case could be derived from cation passivation, and the latter case could be derived from shell passivation.

3.3 Conclusion

Highly stable and luminescent Cd-free InP/GaP/ZnS QDs with a maximum quantum yield of 85% were synthesized by the in situ method. The GaP shell rendered passivation of the surface and removed the traps. TEM images showed a size change. In the TCSPC study, we were able to study the charge transfer dynamics depending on the condition of lattice mismatch by time-correlated single photon counting (TCSPC). As shown in the results, the amplitude of the slow decay component increases as shell structure is added to the InP core which may have been mainly affected by the changes in the surfaces of colloidal QDs to enhance the rate of radiative recombination. This is apparent in previously reported studies involving InP and ZnS core shell structures. The surface traps sites removed by passivation resulting in greater amplitude of the slow decay component. In this study, the main difference is in the cations exchange between indium and gallium ions which not only reduces the surface trap sites but also contributes to the stability of the QDs by reducing the lattice mismatch.

4. Femtosecond transient absorption study of Au rod-TiO_2 nanocomposite: Shell-thickness dependence of charge transfer dynamics

4.1 Introduction

In an effort to expand the optical window for photo catalysis, Au nanoparticles have been used as a sensitizer in a composite material with photo catalytic semiconductors since the absorption wavelength of Au can be tuned by controlling the size of Au nanoparticle.[22] Although the charge transfer dynamics from semiconductor to metal is well known, the charge transfer from metal to semiconductor is not as clearly understood. To better understand this phenomenon, we investigated Au rod-TiO_2 nanocomposite of core-shell type with a range of shell thickness. Using transient absorption spectroscopy, we studied the forward electron transfer from TiO_2 to Au rod as well as the reverse electron transfer from Au rod to TiO_2 as we varied the TiO_2 shell thickness.

4.2 Results and Discussion

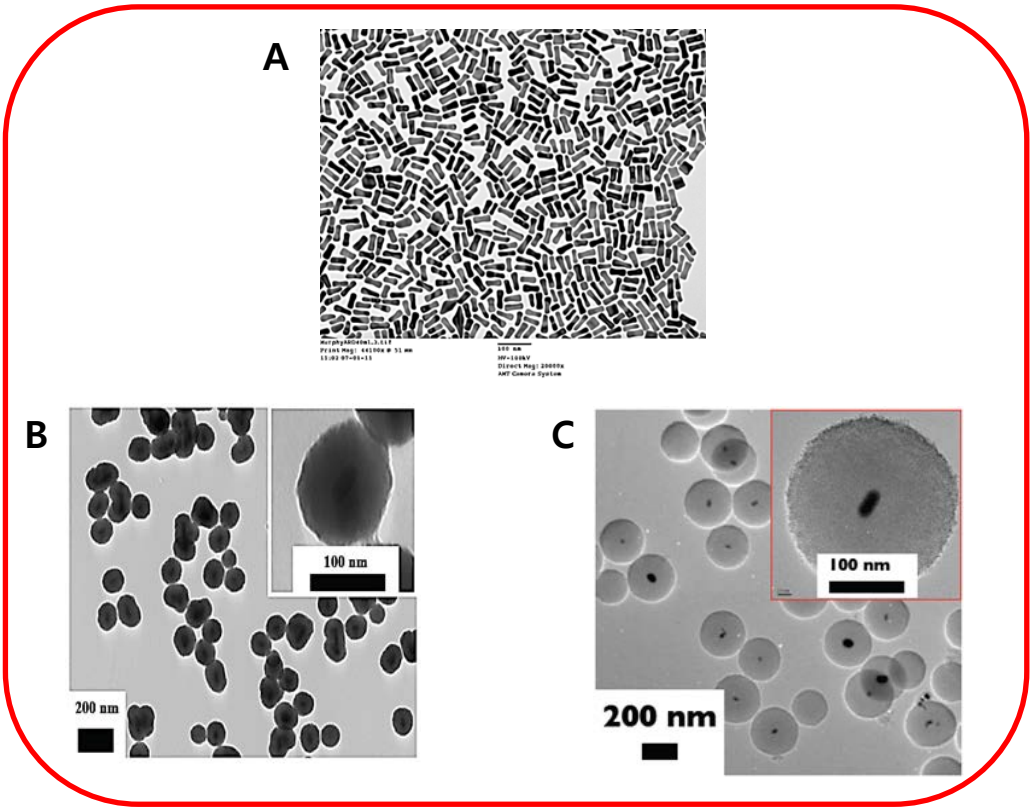

Figure 14. (A) TEM image of Au rod nano structure. (Long axis 40nm) (B) TEM image of Au rod/TiO_2 structure. The size of TiO_2 shell is about 90nm (C) TEM image of Au rod/TiO_2 structure. The size of TiO_2 shell is about 200nm. The size of Au rod in both (B) and (C) is 40nm

Figure 14 shows TEM images of Au rod only, Au rod/TiO_2 (90nm) and Au rod/ TiO_2 (200nm). Figure 14 (B), (C) represent different size of TiO_2 core shell, the same size of Au rod nano composite exists inside of TiO_2 shell. Each shell has single Au rod particle.

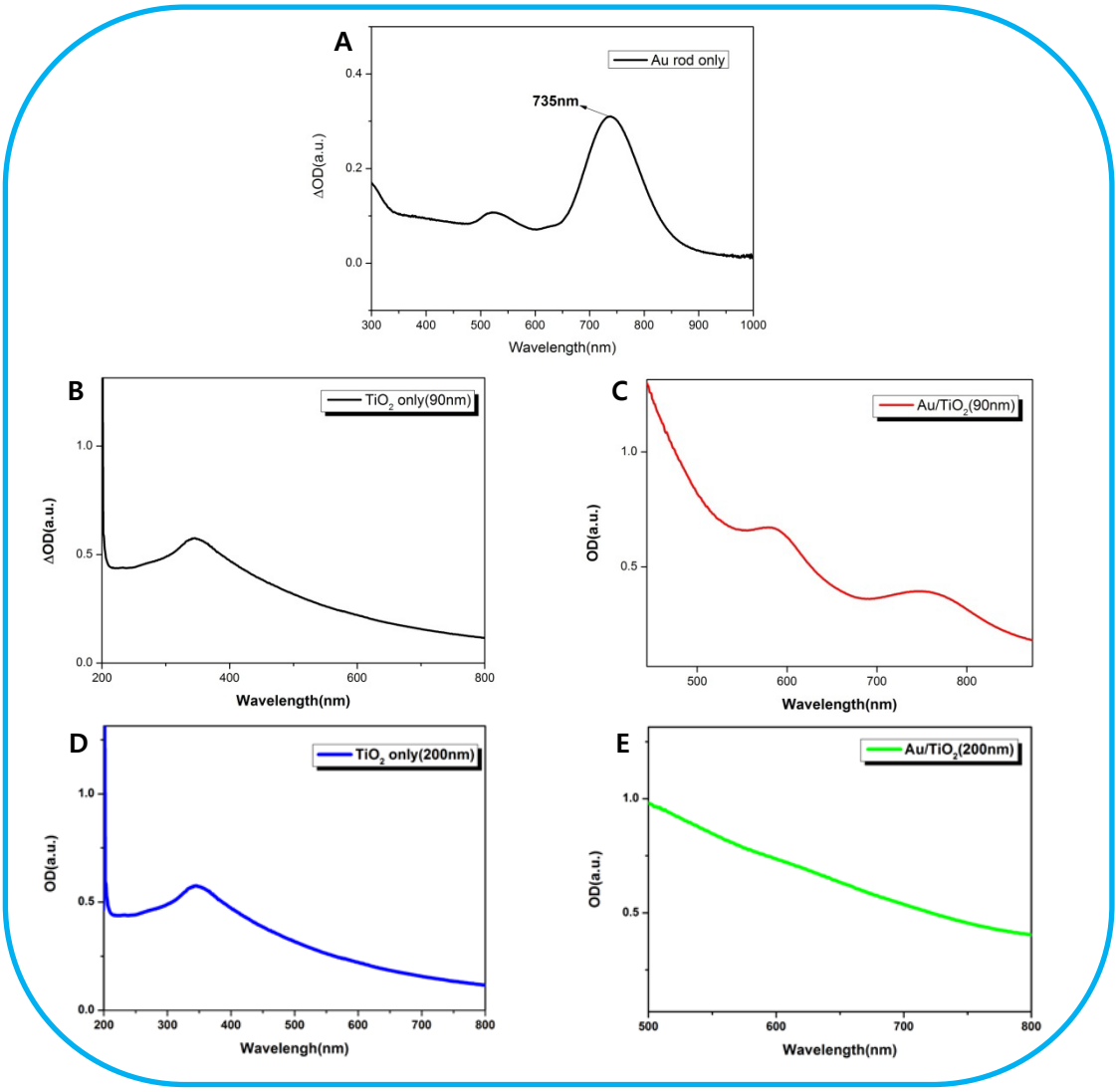

Figure 15. (A) UV absorption spectra of Au rod only in EtOH. (B) UV absorption spectra of TiO_2 only (90nm) (C) UV absorption spectra of Au rod/TiO_2 (90nm) in EtOH. (C), (D) UV absorption spectra of TiO_2 only (90nm) and Au rod/TiO_2 (200nm) in EtOH.

Figure 15 shows UV absorption spectra of TiO_2 only, Au rod/TiO_2 in EtOH as the different shell thickness of TiO_2. Au rod has maxima absorption band (735nm) derived from SPR phenomena. Another short wavelength (530nm) also results from SPR.[23] Absorption spectra of TiO_2 have only UV ranges of wavelength.[24] But, core shell structure of TiO_2 has SPR band which gives potential of photo catalytic effect in visible(near IR) range of light. Figure 15 (E) does not show SPR band of Au rod because of scattering factor of nano structure in UV absorption spectra. However, core shell structure of TiO_2 (200nm) solution shows bluish green color which proves that it absorbs visible (near IR) range of light.

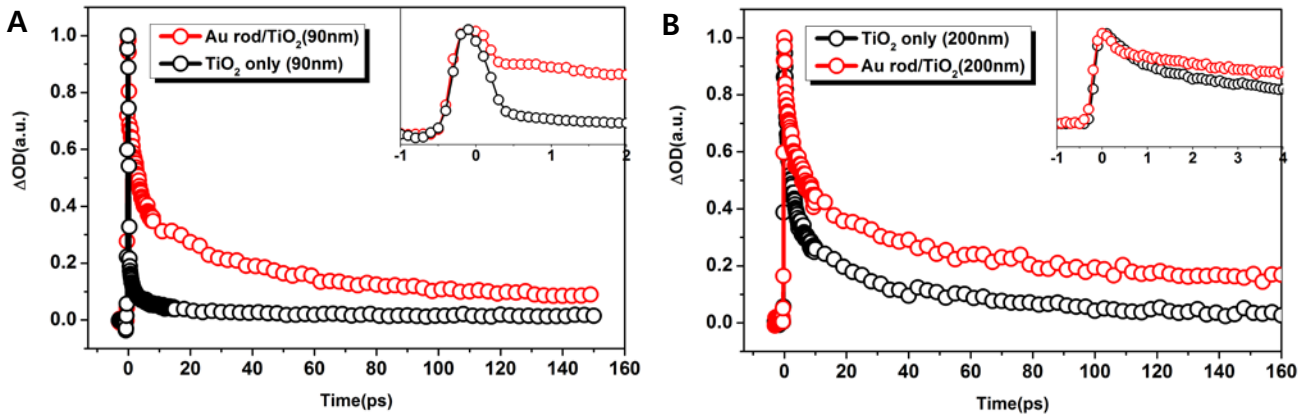

Figure 16. Transient absorption spectra of TiO_2 core, Au rod/TiO_2 core shell as different shell thickness of TiO_2 Pump pulse is at 267 nm and probe pulse is at 850 nm.

We confirmed the visible (near IR) absorption of Au rod/TiO_2 core shell structure exits above (Figure 15). To verify the electron transfer dynamics between Au rod and TiO_2, we used transient absorption technique. Since TiO_2 core has only UV range of absorption, there is no TA (transient absorption) signal in visible (near IR) pump. So, we obtained TA signal in UV pump pulse (267nm). Au rod/TiO_2 core shell has visible (near IR) absorption which could excite electron to move to higher states. Electron dynamics in both cases are probed at wavelength (850nm).

Between TiO_2 and Au rod/TiO_2, there is significant difference in decay curve of TA at UV region. Au/rod TiO_2 core shell shows slow decay curve compare to TiO_2 core case. This means Au rod nano composite affects electron dynamics in excited state of TiO_2.[25] In general, Nano metal could influence on electron movement in excited state of TiO_2.[26] Same phenomena are observed in different shell thickness of TiO_2 and Au rod/TiO_2 (200nm).

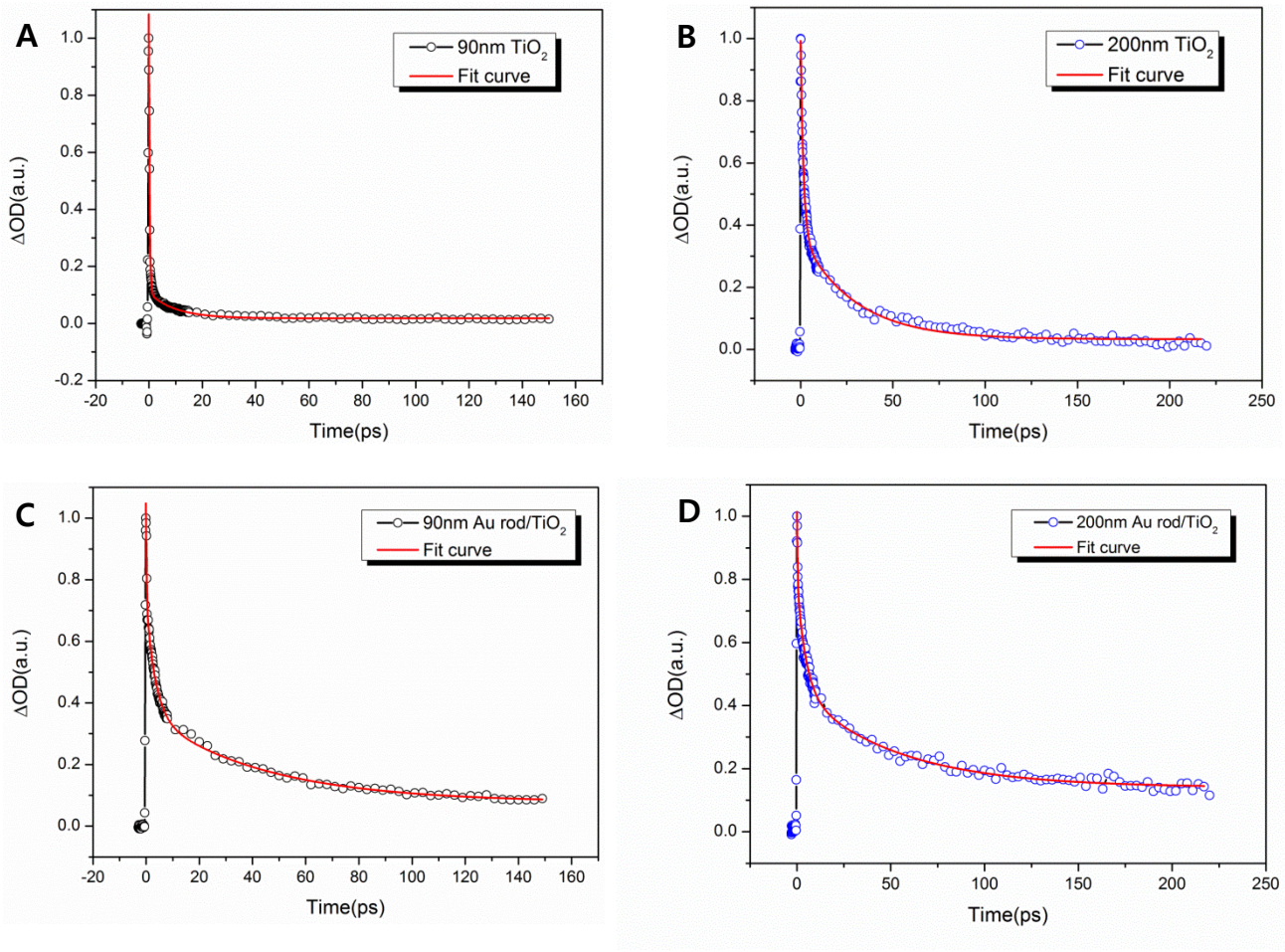

Figure 17. Pump-probe transients of TiO_2, Au rod/TiO_2 at a pump wavelength of 267 nm and probe wavelength of 850nm. The transient decay curve was well fitted by an exponential-decay function.

	T1 (ps)	T2 (ps)	T3 (ps)	Fit function
90nm TiO_2	0.3	10		Bi expdecay2
90nm Au/TiO_2	0.3	44	3.4	Tri expdecay3
200nm TiO_2	1.5	29		Bi expdecay2
200nm Au/TiO_2	0.3	52	4.8	Tri expdecay3

Table 1. Time constants associated with the relaxation of the excited state of TiO_2 and Au rod/TiO_2 in various shell thickness of TiO_2

Figure 17 is transient absorption spectra of TiO_2 and Au rod/TiO_2 in UV region fitted by exponential decay function. We used bi-exponential decay fit with TiO_2 core and tri-exponential decay fit with Au rod/TiO_2 core shell.

$$y = y0 + A1*\exp^{(-(x-x0)/t1)} + A2*\exp^{(-(x-x0)/t2)} \quad \text{where} \quad A1+A2=1$$

$$y = y0 + A1*\exp^{(-(x-x0)/t1)} + A2*\exp^{(-(x-x0)/t2)} + A3*\exp^{(-(x-x0)/t3)} \quad \text{where} \quad A1+A2+A3=1$$

Overall decay of TiO_2 core is fast rather; decay of Au rod/TiO_2 is slower in all shell thickness of TiO_2. As shown in Table 1, each T1 value of cores is almost the same, which results from the thermal relaxation or vibration relaxation of electron in excited states of TiO_2, but T2 value increases from10(ps) to 44(ps) in 90nm TiO_2 and 29(ps) to 52(ps) in 200nm TiO_2. Those of life time result from charge recombination in excited state of TiO_2.[27] Another value of T3 (3.4ps, 4.8ps) are derived from electron in conduction band of Au rod which recombines with hole in valence band of Au rod.[28] These phenomenon could explain Au rod nanocomposite affects charge recombination dynamics of TiO_2. In general, it is well known that charge separation of TiO_2 is short. In our experiment, however, Au rod/TiO_2 system has a longer charge separation time than TiO_2 core, expecting in better photo catalytic effect.

We also see the different decay curves between 90nm TiO_2 and 200nm TiO_2 core in transient absorption spectra. It is interesting that the charge recombination dynamics could be influenced by size of TiO_2. The difference in the recombination rate between TiO_2 (90nm) and TiO_2 (200nm) may be due to the difference in the effective mobility of electron. Once TiO_2 absorbs UV light, electron in ground state of TiO_2 is promoted to its excited state. Generally, this electron loses its energy to surroundings and then charge recombination dynamics occur.

From our data, this motion of electron could be influenced by size of TiO_2. We did not confirm how size of shell has an effect on electron-hole recombination of TiO_2, but this motion of electron is the rate-limiting process for electron-hole recombination in TiO_2. We might little explain the correlation between charge recombination dynamics and size of TiO_2. The data shows that the recombination rate of TiO_2 is decreases as the size of TiO_2 increases. Below, we describe the possible path way of electron in TiO_2.

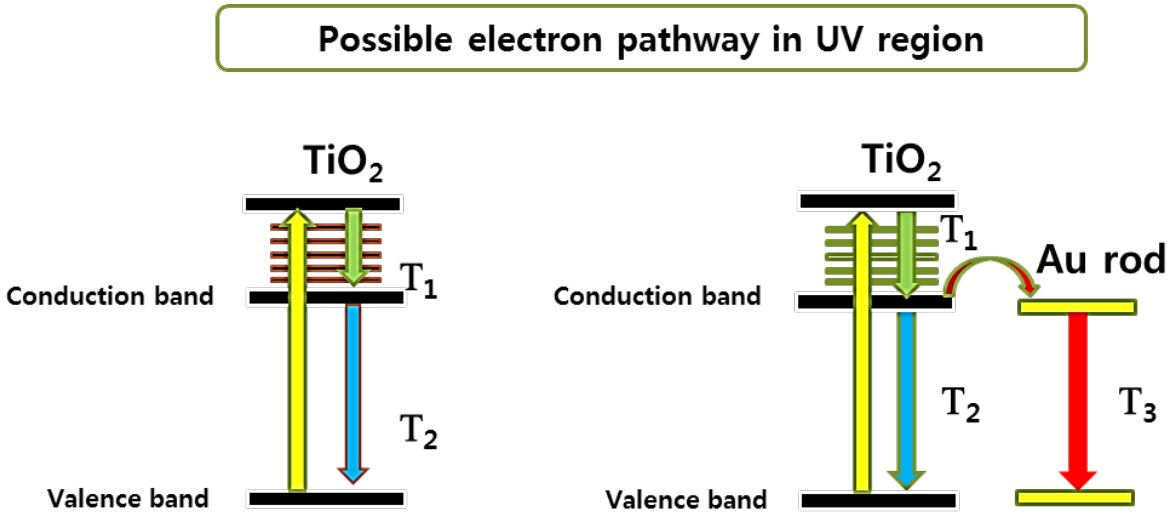

Figure 18. Graphical representation of electron transfer dynamics of TiO_2 and Au rod in UV region

4.3 Conclusion

Charge equilibration between photo irradiated TiO_2 and Au nanoparticles has been probed to elucidate the photo catalytic activity of semiconductor-metal nanocomposites.[29] Such a charge distribution between the two systems has a direct influence on the motion of the electron. The difference electron-hole recombination rate could be reflected in greater photo catalytic efficiency. The present study provides mechanistic explanation for the size-dependent charge recombination rate of TiO_2 and Au rod/TiO_2 composite in UV region. We have found that the TiO_2 shell thickness and Au rod have influenced the charge recombination of TiO_2 which will give a clue to understand of the correlation with photo catalytic effect of it. A better understanding of electron-hole recombination dynamics in visible (near IR) region is also important for designing next generation photo catalysts for light-energy conversion. To better understand the correlation between the lifetime changes of TiO_2 composites and photo catalytic efficiency, more researches on photo catalytic efficiency of TiO_2 under UV and visible region are required.

Appendix

1. Water-based Artificial Photovoltaic System by Fluorescence Resonance Energy Transfer between DSSN (+) and Nile Red

1.1 Introduction

We developed a new type of light sensitizers useful for photovoltaic applications. First, we made a light-harvesting system which DSSN+ was tethered on lipid bilayers and Nile red in an alkyl thiol layer. Absorption range of DSSN+ and emission range of Nile red are well overlapped to make fluorescence resonance energy transfer (FRET). DSSN+ system only uses UV range of light thus photo current generation and efficiency of light harvesting is low. We just combine Nile red fluorophore as an acceptor and DSSN+ as a donor in vesicle system. This improves an efficiency of light harvesting and photo current generation. In this manuscript, we characterize the FRET efficiency between DSSN+ and Nile red in vesicle in solution state by transient absorption spectroscopy.

1.2 Results and Discussion

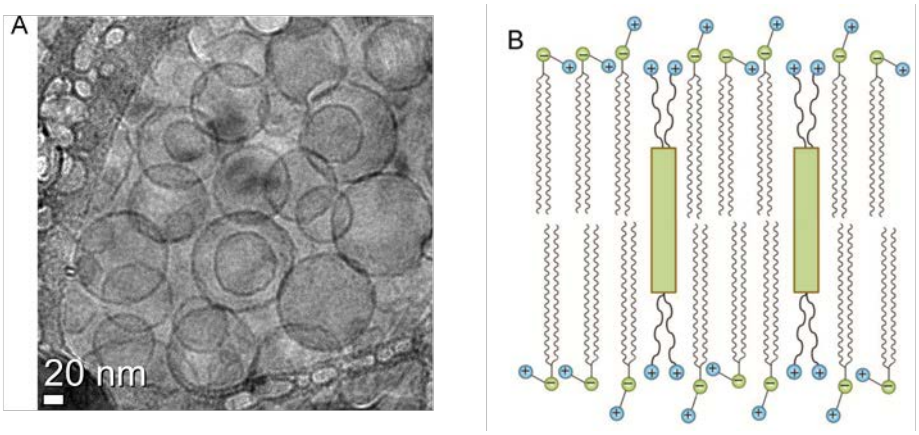

Figure 19. (A) Cryo-TEM image of unilamellar DMPC vesicles bearing DSSN+ relative to lipid. (B) The graphical representation of the phospholipid-assembled DSSN+.

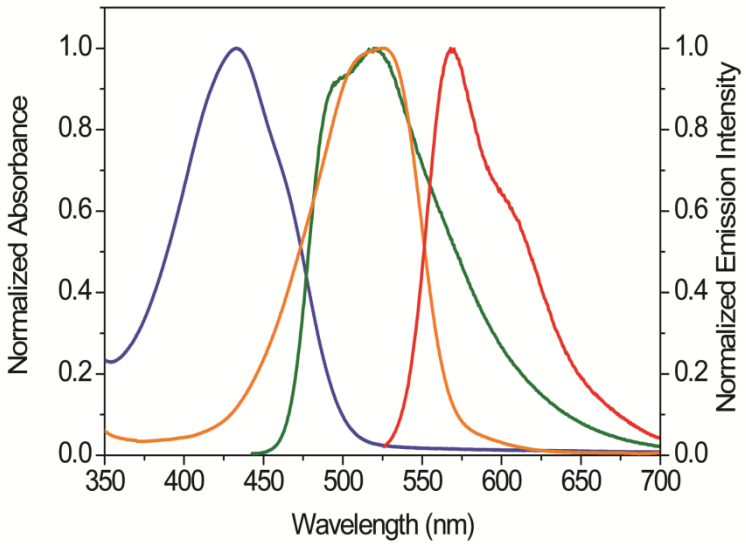

Figure 20. UV absorption and photoluminescence spectra of DSSN+ in lipid vesicles (absorbance = blue, emission = green) and Nile red in toluene (absorbance = orange, emission = red), in which the emission spectrum of DSSN+ is well overlapped with the absorption range of Nile red.

Fluorescence resonance energy transfer (FRET) between DSSN+ and Nile red is verified with steady state photoluminescence (PL) spectra. In Figure 20, DSSN+ has UV range of absorption and visible range of emission. In case of Nile red, this has visible range of absorption. Thus, among these two molecules, energy transfer effectively happens.

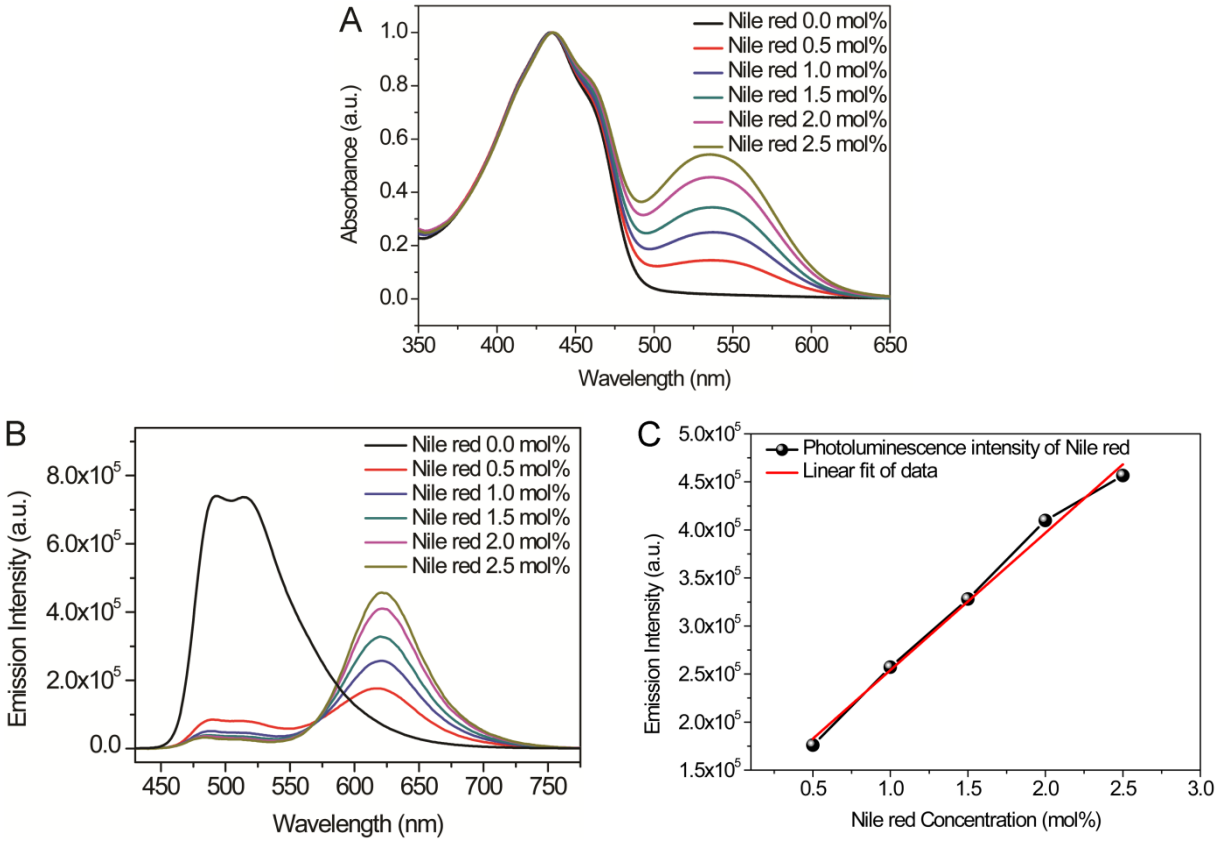

Figure 21. (A) UV absorption spectra of DSSN+ in vesicle solutions as increasing Nile red concentrations at a fixed DSSN+ concentration. (B) Steady state photoluminescence (PL) spectra of the vesicle solutions. The drastic increase in the PL of Nile red excited at 400 nm due to FRET. (C) Linear fitting of the fluorescence maxima at 620 nm with increasing Nile red concentrations.

Figure 21A shows the normalized UV absorption spectra of vesicle solutions in which Nile red absorption constantly increased with concentrations. For these samples, FRET measurements were carried at 400 nm where the donor only absorbed UV range of light and the acceptor absorption could be minimized, evading the excitation of the Nile red directly. Consequently, Nile red emission at 620 nm grows linearly as its concentration is increased. This explains that FRET phenomena take places with effect (Figure 21 B and 21 C).

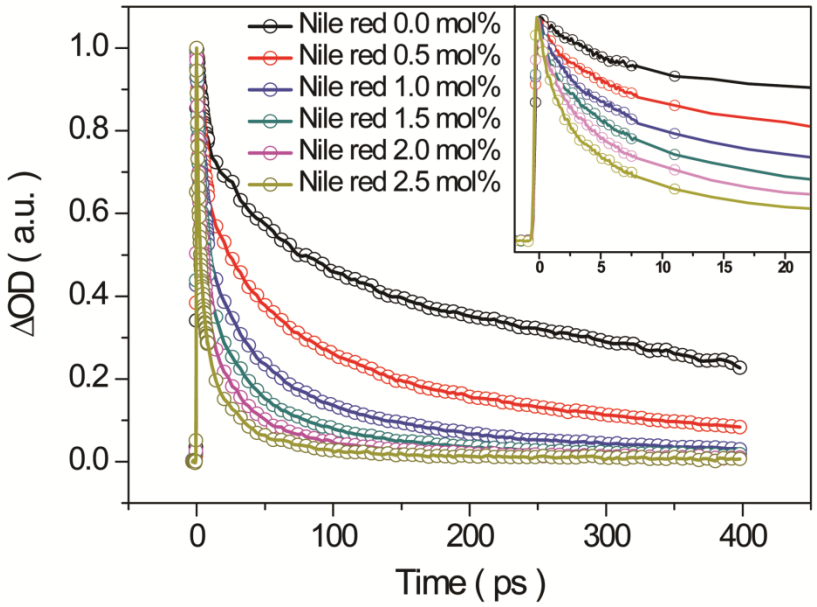

Figure 22. Transient absorption spectra of DSSN+ in vesicle solutions as increasing Nile red concentrations at a fixed DSSN+ concentration.

Table 2. FRET efficiency measured from steady-state PL spectra and transient absorption spectra, and life-time values.

Nile Red (mol%)	FRET Efficiency (E) (Steady-state spectra)	α_1	τ_1 (ps)	α_2	τ_2 (ps)	$<\tau>$ (ps)	FRET Efficiency (E) (Time-resolved spectra)
0.0			11.5		383.4	152.9	
0.5	0.68	0.463	9.2	0.229	171.9	62.9	0.59
1.0	0.84	0.455	6.1	0.212	74.2	27.9	0.82
1.5	0.89	0.458	5.0	0.188	56.5	20.0	0.87
2.0	0.92	0.482	3.5	0.189	37.5	13.1	0.91
2.5	0.93	0.509	2.4	0.186	25.1	8.6	0.94

The FRET efficiency was calculated with steady-state PL spectra and transient absorption spectra (TA)

$$E = \frac{I_A}{I_D + I_A} \text{ and } E = 1 - \frac{\tau_{DA}}{\tau_D}$$

Where I_D is the steady-state PL intensity of the donor in the presence of acceptor, I_A is that of the acceptor in the presence of donor, τ_{DA} is the lifetime of the donor in the presence of the acceptor, and τ_D means that of the donor in the absence of the acceptor. FRET efficiency measured by steady-state fluorescence spectra and transient absorption spectra. In steady-state fluorescence spectra, we observed improvement of fluorescence intensity with the Nile red concentration from 68% at 0.5% mol% up to 93% at 2.5 mol% Nile red concentrations (Table 2).

We also calculated FRET efficiency with life time of DSSN+ and Nile red system. The transient absorption decay curve of donor in the presence of an acceptor has tendency to decrease with increasing acceptor concentration (Figure 22). To estimate the FRET efficiency, we used multi-exponential fit function and FRET efficiency is calculated by average lifetime, $<\tau>=\sum_i \alpha_i\tau_i$.

Here, τ_i means lifetime and α_i is the relative amplitude contribution. Figure 22 shows the TA temporal profiles of DSSN+/Nile red intercalated in vesicles at 400 nm (pump pulse) and 850 nm (probe pulse).

1.3 Conclusion

We have investigated the energy transfer efficiency and photo dynamics between DSSN+ and Nile red. The efficiency of the energy transfer can be improved by adjusting the intercalation ratio between two species in vesicle. The information of lifetime can be used to elucidate energy transfer mechanism and energy transfer rate. By using this information, we are expecting to apply to photo current generation system in future.

References

1. C. Rulliere, Femtosecond Laser Pulses, Springer, Berlin **1998**.

2. S. Mukamel, Principles of Nonlinear Optical Spectroscopy, Oxford University Press, New York, **1995**.

3. Berera, R.; van Grondelle, R.; Kennis, J. T. M. *Photosynth Res* **2009**, 101- 105.

4. McQuarrie, D. A, Simon, J. D. *Physical Chemistry: A Molecular Approach*; 1st ed.; University Science books: Sausalito, CA, **1997**.

5. W. Humbs et al. *Chemical Physics.* **2000,** 254, 319-327

6. *Rev. Sci. Instrum.***2006,** 77, 113105

7. Klimov, V. I. *Annu Rev Phys Chem.* **2007,** 58, 635

8. Alivisatos, A. P. *Science.* **1996,** 271, 933

9. Nirmal, M.; Dabbousi, B. O.; Bawendi, M. G.; Macklin, J. J.; Trautman, J. K.; Harris, T. D.; Brus, L. E. *Nature*. **1996,** 383, 802

10. Reiss, P.; Protiere, M.; Li, L. *Small.* **2009,** 5, 154

11. Ryu, E.; Kim, S.; Jang, E.; Jun, S.; Jang, H.; Kim, B.; Kim, S. W. *Chem Mater.* **2009,** 21, 573-575

12. Xu, S.; Ziegler, J.; Nann, T. *J Mater Chem.* **2008,** 18, 2653

13. Reiss, P.; Protiere, M.; Li, L. *Small*. **2009,** 5, 154

14. Battaglia, D.; Peng, X. *Nano Lett.* **2002**, *2*, 1027–1030

15. Adam, S.; Talapin, D. V.; Borchert, H.; Lobo, A.; McGinley, C.; de Castro, A. R. B.; Haase, M.; Weller, H.; Moller, T. *J. Chem. Phys.* **2005**, *123*, 080706

16. *Appl. Phys. Lett.* **2006,** 88, 123102

17. (a) Son, D. H.; Hughes, S. M.; Yin, Y.; Alivisatos, *A. P. Science* **2004**, 306, 1009−1012 (b) Chan, E. M.; Marcu, M. A.; Fakra, S.; Naggar, M. E.; Mathies, R. A.; Alivisatos, *A. P. J. Phys. Chem.* A **2007**, 111, 12210−12215 (c) Robinson, R. D.; Sadtler, B.; Demchenko, D. O.; Erdonmez, C. K.; Wang, L.; Alivisatos, *A. P. Science* **2007**, 317, 355−358 (d) Wark, S. E.; Hsia, C.; Son, D. H. *J. Am.*

Chem. Soc. **2008**, 130, 9550−9555

18. Park, J.; Kim, S.-W. *J. Mater. Chem.* **2011**, 21, 3745−3750

19. (a) Klimov, V. I.; McBranch, D. W.; Leatherdale, C. A.; Bawendi, M. G., Electron and hole relaxation pathways in semiconductor quantum dots. *Phys Rev B.* **1999,** 60, 13740-13749 (b) Wang, X. Y.; Qu, L. H.; Zhang, J. Y.; Peng, X. G.; Xiao, M., Surface-related emission in highly luminescent CdSe quantum dots. *Nano Lett.* **2003,** 3, 1103-1106

20. (a) Bawendi, M. G.; Carroll, P. J.; Wilson, W. L.; Brus, L. E., Luminescence Properties of Cdse Quantum Crystallites - Resonance between Interior and Surface Localized States. *J Chem Phys.* **1992,** 96, 946-954 (b) Zhang, J. Y.; Wang, X. Y.; Xiao, M., Modification of spontaneous emission from CdSe/CdS quantum dots in the presence of a semiconductor interface. *Opt Lett.* **2002,** 27, 1253-1255 (c) Wang, X. Y.; Zhang, J. Y.; Nazzal, A.; Darragh, M.; Xiao, M., Electronic structure transformation from a quantum-dot to a quantum-wire system: Photoluminescence decay and polarization of colloidal CdSe quantum rods. *Appl Phys Lett.* **2002,** 81, 4829-4831

21. Carstensen, H.; Claessen, R.; Manzke, R.; Skibowski, M., Direct Determination of Iii-V Semiconductor Surface Band-Gaps. *Phys Rev B.* **1990,** 41, 9880-9885

22. Vaidyanathan Subramanian, Eduardo E. Wolf, and Prashant V. Kamat *J. Phys. Chem. B.* ***1999,*** 103, 40

23. John B. Asbury, Encai Hao, Yongqiang Wang, Hirendra N. Ghosh, and Tianquan Lian *J. Phys. Chem. B,* **2001,** 105, 45

24. M.A. Henderson, *Surface Science Reports* 66, **2011,** 185–297

25. *J. AM. CHEM. SOC.* 9, **2004,** 126, 15

26. Nick Serpone. *J. Phys. Chem. B,* **2006**, 110, 48

27. N. Serpone, D. Lawless and R. Khairutdinov. *J. Phys. Chem.* **1995,** *99,* 16655-16661

28. Temer S. Ahmadi, Stephan L. Logunov, and Mostafa A. El-Sayed. *J. Phys. Chem.*, **1996,** 100, 20

29**.** Ryuzi Katoh, Akihiro Furube, Toshitada Yoshihara, Kohjiro Hara, Gaku Fujihashi, Shingo Takano, Shigeo Murata, Hironori Arakawa, and M. Tachiya. *J. Phys. Chem.* B **2004,** 108, 4818-4822

국문초록

시분해 분광학 기술은 순간 생성 물질에 대한 광 동역학 및 광 물리적 특성 연구에 이용되어 왔다. 이러한 기술은 빛으로 유도된 순간 생성물의 전자상태에 대한 연구를 수행하고 전자의 전이 상태의 동역학적인 정보를 파악하는 데 필수적이다. 이 논문은 시분해 분광법 기술을 이용하여 양자점과 반도체에 대해서 전하 전달 및 캐리어 완화 과정에 대해서 연구한 내용을 담고 있다.

양자점에 대한 연구는 발광 특성 및 나노 크기의 작은 입자가 가질 수 있는 고유의 특성에 대한 연구가 널리 수행 되어 왔다. 사이즈에 따른 양자제한 효과로 인한 발광 영역의 조절과 그것의 양자 효율을 높이는 연구가 현재 진행되고 있으며, 본 연구는 CdSe 기반의 양자점이 가지고 있는 독성 문제와 낮은 발광 효율 문제를 해결할 수 있는 멀티 쉘 양자점 시스템을 제안 하였다. 그리고 시분해 분광법을 이용하여 멀티 쉘 양자점과 기존의 양자점과의 전하 및 캐리어 전달 과정 동역학 비교 연구를 수행하였다.

Titania는 고유의 다양한 특징 때문에 많은 분야에 이용되어왔고, 또 상당한 연구가 진행되고있다. 하지만 titania는 전구체의 높은 반응성 때문에 균일한 크기의 입자로 합성하기가 쉽지 않다. 대부분 harsh한 조건에서 입자를 합성하며, 그 결과물이 응집 되어 있거나, 다량의 surfactant를 포함하고 있는 경우가 많다. Mild한 조건에서 균일한 입자를 합성한 경우도 있지만 주로 그 크기가 200 nm 이상인 한계를 가지고 있다. 본 연구에서는 mild 한 조건에서, Ethylene glycol 또는 KCl 의 존재 하에 sol-gel method 를 이용하여 크기 조절 가능한 구형 입자를 합성하였으며 그 크기를 100 nm 이하로 줄이는데 성공하였다. 본 연구는 이러한 Titania와 금 로드 나노 입자를 이용한 Visible(near IR)영역에서의 빛의 활용범위를 넓히고 Titania-골드 로드 core shell 구조를 합성하여 Titania와 코어 쉘 시스템 간의 전하 이동 동역학 연구를 수행하였으며, 광분해 효과와 lifetime과의 상관 관계 해석을 시도 하였다.

시분해 분광법의 응용연구로서 물 기반의 태양전지의 구현을 위해 DSSN+ 와 Nile red 라는 두 가지의 다른 파장영역의 빛을 흡수 할 수 있는 색소를 이중 리피드층에 집적하여 DSSN+ 에서 Nile red로의 에너지 전이를 시분해 분광법으로 확인하였다.

주요어: 순간 흡수 분광법, 시간 상관 단일 광자 계수법, 양자점, 반도체.

학번: 2011-20314

Acknowledgements (감사의 글)

2011년 봄 MRD에 처음 들어 오게 된 이후 벌써 2년째가 지나가고 있습니다. 학부 시절엔 실험뿐 아니라 기초적인 파워포인트 및 워드 작성 조차 하는 법을 몰랐던 저에게 있어서 MRD에서의 2년의 시간은 참 값진 것이었다고 감히 말씀 드리고 싶습니다. 군대를 갓 제대하고 난 뒤 한창 진로 문제로 친구들과 고민하고 있을 시절, 저 역시 저에 대해서 생각을 해보게 되었습니다. 과연 나 자신이 하고 싶은 일이 무엇인가 내가 잘할 수 있는 일이 무엇인가 이러한 고민들은 저로 하여금 저 자신을 다시 한번 돌이켜 보게 해주는 계기가 되었고 대학원 진학이라는 결론을 내리게 되었습니다. 처음 MRD에 들어가서 실험실 생활을 하면서 느꼈던 감정은 힘들다 라는 것이었습니다. 선배들부터 주위 실험실 멤버들 사이에서 약간은 딱딱한 그리고 대하기 어려움을 느꼈기에 적응을 잘 할 수 있을까? 라는 걱정이 많이 들었습니다. 그러던 과정에서 TA 팀이라는 곳으로 가게 되었고 거기서 양일승 박사님을 만나게 되었습니다. 양일승 박사님과의 팀 생활을 하게 되면서 꾸지람도 많이 듣고 저 스스로도 답답함을 많이 느꼈지만, 그러한 과정 속에서 제 자신이 점차 발전을 해나고 있다는 것을 느낄 수 있었기에 내심 뿌듯하기도 하였습니다. 비록 지금은 졸업하시고 안 계시지만 박사님께서 평소에 제게 하시던 말씀이 지금도 많이 생각이 납니다. '항상 프로답게 행동하고 생각해라' 어떻게 보면 당연한 말이기도 하지만 덤벙거리고 실수투성이였던 제게 이러한 말은 가슴 깊이 다가왔습니다. 비록 제 스스로가 발전해 나가고 있다고 하지만, 아직 프로가 되기에는 많이 부족한 것 같습니다. 이런 부족한 저를 팀장으로서 믿고 따라와 주는 종우, 정은이, 도익이, 은학이에게도 감사하다는 말을 하고 싶습니다. 그리고 제가 찾아 가면 언제나 밝게 의논 상대가 되어주던 지원, 지웅, 영빈이도 고맙습니다.

실험실의 큰형들이신 현이형과 남두형 항상 제게 조언 많이 해주시고 때론 따끔하게 일침도 놓아주시지만, 후배를 위하는 따뜻한 맘에 저 역시도 많이 배우게 되었습니다. 저랑 같이 입학한 정은이와 형준이 같이 있었기에 실험실 적응이 한결 쉬웠고 이 자리를 빌어 고맙다는 말 전하고 싶습니다. 그리고 다른 후배 분들에게도 여기 다 적지 못하지만 감사하다는 말을 드리고 싶습니다.

제가 실험실 생활을 하면서 어려움에 처하거나 고민거리가 있을 때마다 언제나 열린 마음으로 저를 반겨 주시던 선생님 진심으로 감사합니다. 항상 과학자로서 날카로운 안목으로 실험실 생활에 활기를 주시는 선생님 한편으로는 실험 외적인 부분에서는 마치 저의 아버지처럼 저를 보살펴 주시고 안아주시는 선생님이 계시기에 저뿐만 아니라 실험실 멤버들도 MRD에서 자랑스럽게 생활 할 수 있는 것 같습니다. 인생에 있어서 사람마다 전환점이 온다고들 합니다. 제게 있어서의 전환점은 MRD 실험실에 들어온 시점부터 시작된 것 같습니다. 아직 나아갈 길이 멀고 힘들겠지만, 이러한 MRD에서의 경험은 저로 하여금 훌륭한 밑거름이 되어 보다 높은 곳으로 도약하는 데 큰 도움이 될 것이라 믿어 의심치 않습니다.

논문 심사를 해주신 서정쌍 교수님, 신석민 교수님께 감사 드립니다. 저의 논문 심사 때문에 심사 위원님들을 번거롭게 해 드린 것 같아 죄송하기도 하고 한편으로는 제가 발전할 수 있도록 관심을 가져주셨기에 이러한 경험이 앞으로의 제게 있어서 큰 도움이 될 것이라 믿습니다.

그 외에 예의 없게 굴던 저를 예쁘게 봐주시고 많은 도움을 주시는 김영규 박사님 친형처럼 좋은 말씀 많이 주시는 재근이 형, 용걸이 형 그리고 레이저 관련해서 많은 도움 주신 전길환 차장님께도 감사하다는 말 전하고 싶습니다.

마지막으로 말도 안 듣고 항상 염려만 끼쳐드린 불효 자식이 저의 부모님께 감사하다는 말 드리고 싶습니다. 경상도 분이신 그래서 무뚝뚝하시지만 말없이 저를 응원해 주시는 아버지 너무너무 감사합니다. 정이 많으시고 항상 아들걱정에 잠 못 이루시는 어머니 너무너무 감사합니다. 그리고 내 동생 선철이 취업 준비한다고 힘들어 하는데 바쁘다는 핑계로 많은 도움 되지 못해서 미안하다는 말 전하고 싶습니다. 저희 가족뿐 아니라 MRD 식구 모두 진심으로 감사하고 사랑합니다.

2013년 2월 관악에서

황 선 진